

See discussions, stats, and author profiles for this publication at: <https://www.researchgate.net/publication/349573429>

Recent Advances in High Entropy Alloys: High Entropy SuperAlloys

Chapter · February 2021

DOI: 10.5772/intechopen.96661

CITATIONS

0

READS

138

9 authors, including:



Modupeola Dada

Tshwane University of Technology

18 PUBLICATIONS 28 CITATIONS

SEE PROFILE



Sisa Pityana

Council for Scientific and Industrial Research, South Africa

192 PUBLICATIONS 1,805 CITATIONS

SEE PROFILE



Fatai Olufemi Aramide

Federal University of Technology, Akure

45 PUBLICATIONS 342 CITATIONS

SEE PROFILE

Some of the authors of this publication are also working on these related projects:



Surface modification of Biomedical Ti6Al4V [View project](#)



Insitu Synthesis and Characterization of Mullite-Carbon Refractory Ceramic Composite from Okpella Kaolin and Graphite for high temperature applications [View project](#)

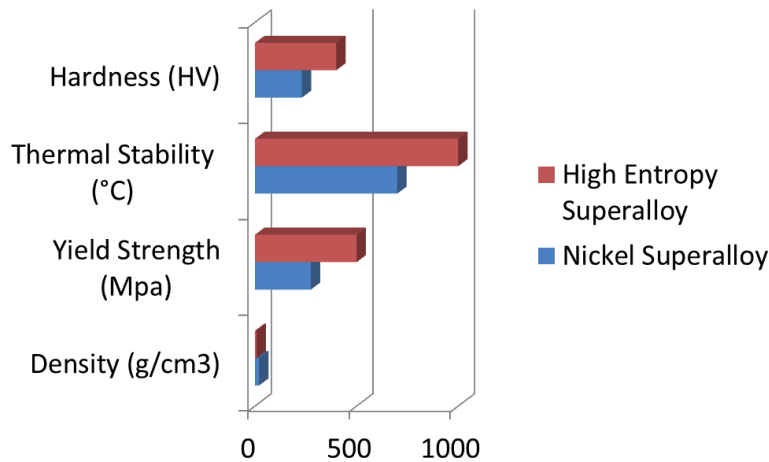
02

Recent Advances of High Entropy

03

Alloys: High Entropy Superalloys

04 *Modupeola Dada, Patricia Popoola, Samson Adeosun,*
05 *Sisa Pityana, Ntombizodwa Mathe, Olufemi Aramide,*
06 *Nicholus Malatji, Thabo Lengopeng and Afolabi Ayodeji*07 **Abstract**08 This study reviews the recent technological advancements in manufacturing
09 technique; laser surface modification and material; High Entropy Superalloys. High
10 Entropy Superalloys are current potential alternatives to nickel superalloys for gas
11 turbine applications and these superalloys are presented as the most promising
12 material for gas turbine engine applications.13 **Keywords:** high entropy alloys, high entropy superalloys, nickel superalloys,
14 turbine engine, laser surface modification15 **1. Introduction**16 Energy transformation comprises the turbine, which is an inner combustion
17 device and a spinning engine that utilizes water, wind steam, helium and air to
18 produce work [1]. Kaygusuz [2] stated that dams use turbines as an electrical
19 generator producing electricity for residential and industrial consumption.
20 Nonetheless, in 1939, the first jet engine that powered an aircraft was built consist-
21 ing of the combustion chamber, the turbine and the compressor [3]. This turbine
22 used air as its working fluid in an internal combustion engine and this engine, in
23 turn, removes enough chemical energy to convert it to mechanical energy from the
24 fuel source while using the working fluid to drive the propeller and the engine [4].
25 Bell and Partridge [5] anticipated that the Joule cycle is a theoretical cycle for gas
26 turbine applications, where both expansion and compression routes take place in a
27 rotating machine [6]. This comprises some reversible processes such as the turbine
28 using the expansion process and fluid friction for an increase in entropy which
29 causes a spontaneous reaction using the compression method in the Brayton cycle
30 [7]. The gas turbine is characterized by extended overhaul intervals, an increased
31 operating speed, less moving parts, availability, low maintenance, reliability, long
32 life span and rugged design [8]. The design of a turbine engine dictates its perfor-
33 mance and the performance requirement are determined by the shaft house power
34 developed in certain temperature conditions which may be extreme. Therefore, the
35 need for high-performance materials becomes necessary because one factor which
36 affects the efficiency of the engine; the turbine inlet temperature is made up of
37 materials which are designed to reduce flow losses and must withstand erosion,
38 corrosion and stress at elevated temperatures [9]. According to Reed [10],



01 **Figure 1.**
02 Comparison graph between nickel super alloy and high entropy superalloy.

03 superalloys especially Nickel Superalloys are materials generally used at elevated
04 temperatures for these gas turbine applications attributed to their elevated tem-
05 perature strength, corrosion resistance, excellent formability, cost and low density
06 [11]. However, the nickel-based superalloy has a maximum service temperature, not
07 over 650 °C attributed to the conversion of γ' precipitate strengthening matrix to
08 the δ phase over time [12]. More so, the nucleation and growth of some cavities
09 along the transverse grain boundaries of these materials are the gas turbine airfoil's
10 failure mechanisms [13]. Therefore; a need to develop new materials with improved
11 properties was necessary and this was achieved by transforming conventional
12 material into new ones via advanced industrial reproduction [14]. Miracle, Tsai [15]
13 proposed High Entropy Superalloys (HESAs) as a new class of amalgam with
14 superior properties compared to traditional superalloys as shown in **Figure 1**.

15 Their elemental composition, lower densities, high configurational entropy and
16 core effects alongside possessing the γ' precipitate reinforcement phase makes this
17 superalloy a preferred alternative material for turbine engine applications [16]. In a
18 previous study, additive manufacturing was presented as a potential advance manu-
19 facturing technique as opposed to conventional arc melting and casting fabrication
20 processes. This study attempts to present HESAs as a promising material for gas
turbine engine applications, as opposed to traditional Nickel-based superalloys [17].

21 **2. Advances in material development**

22 **2.1 Super alloys**

23 Superalloys are stable materials; they do not oxidize or fall apart in very harsh
24 environments and at high temperatures. These amalgams are used for power
25 generation, industrial, marine and aerospace applications [10]. They are character-
26 ized by their excellent heat and oxidation resistance at elevated temperatures, high
27 melting temperature, and high-temperature mechanical strength, good fracture
28 toughness, and stress-rupture, creep resistance [18]. In general, superalloys contain
29 more of Co, Ni, Cr or Fe but less of Ta, Hf, W, Cr, B, Mo, Nb, Al, Zr, C, Ti because
30 these elements adversely affect the properties of the blend. Superalloys have a
31 typical face-centred cubic structure and are characterized by a γ' precipitate with
32 operating temperatures above 600 °C [19]. This phase gives the superalloy a

01 principal yield strength which increases with a temperature rise. They may have
02 equiaxed or columnar grain structures without exhibiting high-angle grain bound-
03 aries, which at high temperatures are sites for damage accumulation [20]. According
04 to Graybill, Li [21], Superalloy's strengthening mechanism includes dispersion
05 strengthening, solid solution and precipitation strengthening [22]. The dispersion
06 of chemically inert carbides and nitride enhances the strength of the superalloy.
07 Precipitation of all intermetallic phases, namely; carbides and FCC matrix γ'
08 precipitate enhances the strength of the superalloy through Ti, Cb, Ta and Al, which
09 promote the formation of the γ' precipitate. Finally, solid solution strengthening
10 with tungsten, columbium, rhenium, molybdenum, rhenium and tantalum stabi-
11 lizes the FCC structure and strengthens the superalloy [23].

12 Gessinger and Bomford [24] suggested that Superalloys for gas turbine applica-
13 tions are widely fabricated using powder metallurgy. However, Bewlay, Gigliotti
14 [25] fabricated the turbine disks using hot die forging and roll forming. Lavella,
15 Berruti [26] studied the residual stresses in Inconel 718 turbine disks fabricated by
16 milling while Groh, Gabb [27] developed a turbine disk using the casting technique.
17 Compared with these conventional techniques, the powder metallurgy process
18 produces turbine disks which are extremely difficult to forge; die life is relatively
19 poor and die fill is extremely difficult but not with additive manufacturing.

20 2.1.1 Nickel superalloys

21 Gas turbine engines require higher temperatures for efficiency. This high-
22 temperature application, therefore, requires excellent emission control with an
23 advance in the combustion hardware of the engine. Nickel superalloys materials
24 were developed for this purpose and they make up about half of the weight of
25 materials used in turbine engines [28, 29]. They have an FCC nickel matrix which is
26 stable enough for the alloy to be used for combustion liners, blades, vanes, thermal
27 barrier coatings, burners and are also applied to bear loads of over 75% of their
28 emergent melting temperature. This is attributed to their characteristic high-
29 temperature rupture and creep resistance, lifetime expectancy, low operating costs
30 and excellent thermal efficiency [30]. Nickel superalloys are also used in space
31 vehicles, submarines, petrochemical equipment and nuclear reactors. Nickel-based
32 superalloy 718 (IN718) is widely used in wrought or cast at 540 °C for rotors in gas
33 turbine applications [14]. Nickel superalloy 925 and 725 having good corrosion
34 resistance are applied in the oil and gas industry where carbon dioxide, hydrogen
35 sulphide, free Sulfur and chloride levels are significantly high. Nickel superalloy 706
36 (IN706) is used for power generation for its large diameter and lower concentrations
37 of other alloying elements. Alloy 685 (Waspaloy) with high-temperature strength
38 and age hardening is widely used for gas turbine engine applications [31]. The
39 superalloy is resistant to corrosion and oxidation whilst withstanding extreme
40 atmospheric conditions while in service. Other compositions are; Rene N6 used in
41 Jet engines, Inconel Alloy 600 used for stills, condensers, heaters and evaporator
42 tubes. Alloy 601 is used for pollution control, power and aerospace applications [32].
43 Nimonic 90 is used for turbine disc, blades, hot-working tools and forging. However,
44 Nickel-based superalloy is difficult to machine attributed to its hardness, toughness,
45 and they possess high heat resistance at elevated temperatures alongside low thermal
46 conductivity [33]. Machining at high pressure causes work hardening rapidly, which
47 invariably causes the alloy component to warp. Furthermore, Nickel superalloys can
48 be easily replaced with alloys that have high creep strength and niobium silicide was
49 an appropriate system to replace nickel superalloy having 170 MPa creep strength and
50 at a density of 7 g/cm³ until recently. Research showed that the addition of Ru and Re
51 to the nickel superalloy led to the enhancement of the superalloy's creep strength,

01 however; these additions are expensive and cause density inversion which results in
02 the defect [34]. This superalloy's stability is limited at very high temperatures [35].

03 According to Durand-Charre [36], Nickel-based Superalloys are majorly FCC
04 phase structured. However, in aluminum-nickel superalloy systems, a second
05 precipitate phase is formed, which is usually Ni_3Al in a composition containing an
06 ordered intermetallic structure [37]. The γ' phase relies on the cooling rate of the
07 superalloy through the solvus temperature of 894°C [38]. A fast cooling rate
08 promotes a unimodal distribution of the γ' precipitate, therefore, an increasing the
09 volume of the γ' phase through rapid solidification is essential to the strengthening
10 properties of the superalloy [28]. Although the precipitate morphologies can be
11 modified through heat treatment and other secondary phases observed in Nickel-
12 based superalloys are ordered FCC γ' , FCC carbides, ordered body-centred tetrago-
13 nal γ'' and ordered orthorhombic intermetallic phases [39].

14 Pollock and Tin [28] did an intensive review on nickel superalloys and the
15 authors stated that the commercial superalloys comprise Co, Cr, W, Mo, Ta, W, Nb,
16 Re, Ti, Al, C, Hf, Y, B and Zr. The yield strength of the nickel superalloy is between
17 $900\text{--}1300$ MPa at room temperature and the fatigue life at 593°C is 600 MPa at
18 10^6 cycles and 10^9 cycles. Additions of Re, Nb, W and Mo can be added for the solid
19 solution strengthening of the superalloy. Y, Ta and Cr contribute to enhance the
20 corrosion and oxidation properties of the superalloy. While Zr, C, Hf and B are
21 carbides or borides forming agents that help enhances the mechanical properties of
22 the superalloy as they are situated at the grain boundaries. The creep rupture life
23 attains about 1100°C at 137 MPa stress level after 1000 h which is about 90%
24 fraction of the melting point signifying the need for innovative advanced materials
25 having higher melting points for the hottest regions of the turbine engine.

26 *2.1.2 High entropy superalloys (HESAs)*

27 Throughout the years, alloys utilized for commercial reasons were structured
28 by choosing an element which framed the network of the whole component with
29 the addition of essential solutes to the base component [40, 41]. The blends of
30 these combinations were reduced as could reasonably be expected for the immense
31 development of mass intermetallic mixes existing within the molar atomic pro-
32 portions of these alloys, hence, attaining a 40% mark or more. Along these lines,
33 the intermetallic phases reduce the quality of the alloys while in service [42, 43].
34 Therefore, a need arose to search for alloys with atomic percentages lesser than
35 35% and the possibilities of combining many metallic principal elements in several
36 atomic compositions were further investigated [44]. According to Ye, Wang [45], an
37 innovative class of alloys with these attributes was discovered more than a decade
38 ago by mixing multiple principal elements in equimolar or near-equimolar compo-
39 sitions. Yeh, Chen [46] named the alloys 'High Entropy Alloys' (HEAs). The authors
40 defined HEAs as amalgams having compositions with at least five principal metallic
41 elements, with these components having a molar atomic proportion between 5 and
42 35% [47]. Studies on HEAs have concluded that most HEAs comprise simple FCC,
43 BCC or HCP solid solutions phase attributed to their high-entropy effect [48].
44 Wang, Li [49] suggested that these solid solution phases with little or no intermetal-
45 lic matrix enable HEAs to have outstanding properties such as strength, extraordi-
46 nary mechanical and physical properties at cryogenic temperatures, plastic strain,
47 fracture strength and good ductility; they possess elevated-temperature oxidation
48 resistance and excellent work hardenability and have been reported to possess dis-
49 tinctive magnetic and tribological properties [50, 51]. Furthermore, Senkov, Wilks
50 [52] reported that HEAs are exceptional refractory materials and their fatigue-
51 resistance were reported to exceed conventional alloys by Hemphill [53].

01 In the literature, the development in the solid solution strengthening of High
02 Entropy Alloys (HEAs) and the precipitation hardening properties of the alloys at
03 temperatures above 1100 °C, led to the discovery of High Entropy Superalloys
04 (HESAs). Yeh, Tsao [17] stated that these superalloys are simply HEAs with the bulk
05 of γ' precipitates and they are described by their high elongation at room tempera-
06 ture, compressive strength, lower densities, creep resistance and ultimate tensile
07 strengths at elevated temperatures. Tsao, Yeh [54] suggested that High Entropy
08 Superalloy (HESA) is made up of a first elemental content containing at least
09 35 at.% and each principal reinforcement elemental combination will have a second
10 elemental content of more than 5 at%, for example, $\text{Ni}_{40.7}\text{Al}_{7.8}\text{Cr}_{12.2}\text{Fe}_{11.58}\text{Co}_{20.6}\text{Ti}_{7.2}$
11 HESA. Senkov, Isheim [55] developed a refractory high entropy superalloy and the
12 authors anticipated that the first and second elemental composition content is
13 derived by the mixing entropy of more than 1.5 R (R is the ideal gas constant)
14 alongside the principal strengthening elemental composition, respectively.

15 Chen, Chang [56] studied the hierarchical microstructural strengthening of
16 HESAs and the composition of strengthening elements can consist of Cu, Fe, Ti, Zr,
17 Co, V, Al, Nb, Cr and Mn. While the overall structure can comprise Mn, Ni, Fe, Ti,
18 Co, Cr and V while for the grain boundary strengthening; C, B and Hf are added
19 but must not be over 15% of the superalloy's total compositional weight. Refractory
20 elements like Ru, Ta, Re, Mo and W can be added but must also contain less than
21 15% of the total superalloy's weight [55]. Tsao, Yeh [57] in 2013 recommended the
22 development of superalloys using HEAs microstructure with single phases and
23 an additional second phase for elevated temperatures applications. Yeh, Tsao [17]
24 then fabricated $\text{Ni}_{40.7}\text{Al}_{7.8}\text{Co}_{20.6}\text{Cr}_{12.2}\text{Fe}_{11.5}\text{Ti}_{7.2}$ high entropy superalloy (HESA) via
25 casting method. The authors reported that the microstructure of the composition
26 was stable at elevated temperatures and the superalloy was made up of γ' nanosized
27 precipitates with a density lower than 8 g/cm³.

28 Daoud, Manzoni [58] developed $\text{Al}_8\text{Co}_{17}\text{Cr}_{17}\text{Cu}_8\text{Fe}_{17}\text{Ni}_{33}$ HESA using thermos-
29 calc, the authors compared the results with Alloy 800H and IN617. They reported
30 that the HESA had higher tensile strength, this was attributed to two phases; one
31 spherical γ' precipitate which was less than 20 nm after the aging temperature at
32 700 °C and another less than 350 nm with an elongated morphology. He, Wang [59]
33 fabricated $\text{Fe}_{9.4}\text{Co}_{9.4}\text{Ni}_{9.4}\text{Cr}_{9.4}\text{Ti}_2\text{Al}_4$ HESA with γ' nanosized precipitates to manipu-
34 late the thermomechanical properties of HESAs, and they argued that the superal-
35 loy had γ' nanosized precipitate with an outstanding yield strength and elongation
36 [60]. According to Xiao, Gregoire [61], scanning alternating current calorimetry
37 can be used to quantify the thermomechanical properties of superalloy.

38 Wang, Zhou [62] investigated $\text{Al}_{0.2}\text{CrFeCoNi}_2\text{Cu}_{0.2}$ HESA and discovered the γ'
39 nanosized precipitate with 30% elongation. Tsao, Yeh [57] developed seven HESAs
40 using the elements Ni, Fe, Al, Cr, Co, Ti by vacuum arc melting. They stated that the
41 development of the γ precipitates in the superalloy was due to Fe, Cr elements and
42 the γ' matrix, they stated that substituting Ni with Ti enhances the thermal stability
43 of HESAs thus encouraging the γ' matrix and by controlling the elemental compo-
44 sitional partitioning in the middle of the γ - γ' phase, the thermal properties of the
45 high entropy γ matrix can be improved. More so, at elevated temperatures after long
46 term exposures L_{12} γ' nanosized precipitates were formed without topological
47 closed packed phases. Gwalani, Soni [63] examined $\text{Al}_{0.3}\text{CoCrFeNi}_2$ and
48 $\text{Al}_{0.3}\text{CoCrFeNi}$ HESAs and the authors observed γ' precipitate in the $\text{Al}_{0.3}\text{CoCrFeNi}$
49 super alloy until 550 °C but were replaced with a B2 phase at 700 °C after annealing
50 attributed to the increase in aluminum content [64].

51 Senkov, Isheim [55] and Li, Lee [65] tested $\text{AlMo}_{0.5}\text{NbTa}_{0.5}\text{TiZr}$ HESA by powder
52 metallurgy and they all observed that the superalloy possessed high thermal stabil-
53 ity and yield strength superior to nickel superalloys at 1200 °C. Kai, Cheng [66]

01 examined the oxidation behavior of a HESA in O₂ environments. The
02 Ni₂FeCoCrAl_{0.5} HESA oxidation kinetics at 900 °C followed a parabolic-rate law
03 forming scales which was dependent on the oxygen pressure. The results showed
04 that the oxidation rates increased with an increase in oxygen pressure however, the
05 kinetics of mass-loss was observed. Shafiee, Nili-Ahmadabadi [67] designed a
06 wrought HESA using Phacomp and CALPHAD technique. The reports showed that
07 the superalloy comprised of γ' nanosized precipitates with lower densities, excel-
08 lent workability and high thermal stability than Inconel 718 alloy and Waspaloy.
09 Saito, Chen [68] discussed the influence of heat treatments on HESA microstruc-
10 tural evolution and results showed the cast HESA had coarsened γ' precipitates
11 attributed to microsegregation which decreased the solidus making the γ' solvus
12 unclear. Finally, Zhang, Huo [69] prepared cast Ni_{48-x}Co₁₈Fe_{9.3}Al_{9.7}Cr_{10.5}Ti_{4.5}Mo_x
13 HESA to investigate the mechanical and microstructural properties of the superal-
14 loy and they concluded that HESAs exhibits good compressive strength at elevated
15 temperature, elongation and tensile strength at room temperatures than nickel
16 superalloy.

17 HESAs are stable at elevated temperatures compared with commercial Rene' N6,
18 Udimet 700 and Hastelloy X superalloys, this attributed to their sluggish diffusion
19 and high entropy effect. At high temperatures, Nickel-based superalloys form
20 intermetallic topological closed-packed (TCP) phases rich in Fe-Cr because of the
21 high iron content in less than 100 h at 900 °C and this TCP phases formed is
22 detrimental to the stability of superalloys at high temperatures [70]. However, at
23 900 °C in more than 200 h, there was no TCP phase observed in Ni_{40.7}Al_{7.8}Cr_{12.2}
24 Fe_{11.58}Co_{20.6}Ti_{7.2} HESA and the γ - γ' microstructure of the superalloy remained stable
25 after isothermal aging for 500 h at 1050 °C [57]. The elevated temperature strength
26 of HESAs has been reported to be higher than that of IN 617. This can be attributed
27 to enhancing the APB energy, increasing the lattice distortion and/or adding
28 refractory Ta and W elements in high concentration to the compositional system.

29 Yeh and Tsao [71] did a thorough analysis of HESAs with the elemental composi-
30 tion of Fe, C, Al, Mo, Cr, Ti, Ni, Co, Ta, W and Nb. The siderophile element was
31 Nickel while the strengthening element was Nb and C. The authors reported that the
32 HESA's microstructure comprised an FCC, L12 crystal structure and γ' phase while
33 the superalloys had hardness values of 400–470 HV at room temperature. At ele-
34 vated temperatures, the HESAs hardness values recorded were between 300–350 HV.
35 These values are greater than IN718 under high temperature. The yield strength of
36 HESA at 1000 °C was about 500 MPa. At a strain of 150 MPa under a temperature
37 of about 980 °C, the HESAs showed excellent elevated temperature creep strength
38 when compared with first generational superalloys. The creep strength and fatigue
39 resistance of HESAs is due to the positive lattice misfit of the superalloy [72]. The
40 raft which directionally coarsens the γ' precipitate is corresponding with the stress
41 axis which results in a sluggish motion of dislocation in the γ - γ' precipitate inter-
42 face, thus hindering the propagation of cracks initiated by fatigue and perpendicu-
43 lar to the same stress axis [73]. The HESAs showed promising thermal stability with
44 a compact protection layer of Cr₂O₃, Al₂O₃ observed on the surface of the HESAs at
45 elevated temperatures, while the densities of the HESAs ranged from 7.78–7.94 g/
46 cm³ as opposed traditional superalloys that range between 7.8–9.4 g/cm³ attributed
47 to the high concentration of Cr, Fe, Ti and Al elements [42]. Other superalloys used
48 for turbine engine applications are presented in **Table 1**.

49 **2.2 Protection of superalloys in gas turbine applications**

50 Wee, Do [81] described in a review of the mechanical thermal properties of
51 superalloys and the authors stated that superalloys are required to perform excel-
52 lently under severe thermal and mechanical stresses. The turbine engine may

SuperAlloy	Composition	Phase Structure	Advantages	Disadvantages	Ref
Iron-Based (Incoloy 800H, Type A-286 alloy, IN903)	IN800H (32Ni-21Cr- 1.5Mn-01Si- 0.3Ti-0.3Al-01C- bal Fe, wt.%)	γ and γ'	Room- temperature strength, high- temperature strength, Creep, Wear and oxidation resistance	Difficult to machine, poor service performance, susceptible to defects, hot corrosion degradation	[74–76]
Cobalt-Based	(Co-30Ni-11Al- 2Ti-5.5 W-2.5Ta- 0.1B, at%)	γ, γ' and TCP	High strength at elevated temperatures, corrosion -resistant, thermal shock resistant, easy to machine	Low strength compared to other superalloys,	[77, 78]
Titanium- based (TiAl, Ti6Al4V)	(Ti-48Al-2Cr- 2Nb)	γ , FCC L1 ₂	High Strength- toughness and fatigue strength, corrosion- resistant,	Low adhesive, high friction coefficient, low ductility	[79, 80]

01

Table 1.
Superalloys used for turbine engine applications.

02 experience failure attributed to linear and cyclic movements of the pistons, con-
 03 necting rods, rotors and shafts majorly affecting the cascade fluids on the surface of
 04 the superalloy [82]. For turbine applications, superalloys comprise elements which
 05 are meant for elevated temperature strength required for efficiency [83]. However,
 06 these alloying elements may also adversely impact the superalloy's resistance when
 07 in this severe environmental conditions over some time. Therefore, there may be a
 08 need for additional protection of the superalloy through surface treatments [84].
 09 There are several laser surface modification treatments, namely; laser surface hard-
 10 ening, laser surface heat treatment, Laser alloying, laser shot peening, laser surface
 11 dispersing and laser coatings and cladding [85]. Laser coatings enable the superalloy
 12 to be resistant to its environment, have microstructural stability and enhance its
 13 thermal, physical and mechanical properties [28, 86]. The coatings available can
 14 be classified as; overlay coatings, diffusion coatings and ceramic barriers [87, 88].
 15 The deposition of Al from a different external source and diffusing it into the base
 16 superalloy to for an external layer is called aluminide or diffusion coating. Bonding
 17 an oxidation-resistant alloy which is weak but highly effective on a superalloy to
 18 enable surface protection and stability is called overlay cladding, while ceramic
 19 barriers are ceramic coatings attached to the surface of a superalloy [89].

20 3. Advances in manufacturing technology

21 Technological advancements in surface engineering have replaced conventional
 22 methods of surface treatments with laser surface modification (LSM) techniques.
 23 The use of lasers in LSM has been reported to produce wear, corrosion, fracture
 24 and fatigue resistant HEAs coatings. This is attributed to the energy absorption and
 25 rapid solidification of the deposition process, which promotes fine microstructures
 26 necessary for surface modification.

01 According to Wu et al. [90] used laser surface alloying to study the phase evolu-
02 tion and cavitation erosion-corrosion behavior of a HEA coating in distilled water
03 and NaCl solution. The study showed that the alloy's cavitation erosion resistance
04 was enhanced in distilled water but not in NaCl solution due to the corrosion.
05 Zhang et al. [91] fabricated HEA by laser surface alloying to examine the properties
06 of the alloy and they reported that the microhardness property of the coating was
07 thrice the number of the substrate and there were improvements in the wear resis-
08 tance of the alloy. Huang et al. [92] investigated an equimolar HEA on a titanium
09 alloy substrate using LSM and the results also showed enhancements in the wear
10 resistance of the alloy attributed to the manufacturing route which contributed to
11 the formation of the phases observed in the BCC matrix. Nahmany et al. [93] used
12 an electron beam surface remelting technique to modify two-five component HEAs,
13 and the authors inspected the influence of these surface modification processes
14 on the properties of the alloys. The authors observed a significant increase in the
15 microhardness due to the rapid solidification and cooling process associated with
16 the fabrication technique. From literature, it can be deduced that LSM classified
17 into laser surface remelting, surface amorphisation, laser transformation harden-
18 ing, shock hardening, laser cladding, laser surface alloying and laser shock peening
19 using different types of lasers can be used to enhance the properties of HEAs [94].

20 **4. Laser surface modification**

21 Laser application in surface modification techniques can be dated back to Albert
22 Einstein who was the first scientist to conceive a stimulated emission in 1917 which
23 today makes lasers applicable [95].

24 A laser is an abbreviation for "light amplification by stimulated emission of
25 radiation". It is classified into CO₂ and Excimer gaseous lasers, Nd:YAG Solid-state
26 Lasers, Liquid Dye lasers and Yb-doped Fiber. These lasers consist of an optical
27 resonator, a pumping energy outlet and a gain medium. The gain medium is located
28 inside the optical resonator which amplifies a light beam using external energy sup-
29 plied by the pumping energy outlet. They are classified into dyes, semiconductors
30 or fibers, solid and gaseous states.

31 Lasers are generally characterized by the ability to avoid divergence in a long-
32 distance, possession of an increased level of energy and monochromaticity [96].

33 a. The CO₂ laser comprises an electric pump, discharge tube, CO₂ gas for the
34 gain medium and optics such as silver or gold mirrors, zinc selenide lens and
35 finally a window as the optical resonator. Although the Helium-Neon laser was
36 the first gas laser developed in a Bell telephone laboratory, still, the CO₂ is the
37 most widely used gas laser for its high emission wavelength between 9–11 μm
38 which offers very high power for surface modification. The process experiences
39 low light absorption in the infrared regions, reduced optical fiber delivery,
40 instability in the output power attributed to the contraction of the laser
41 structure and thermal expansion when pumping the gas by an AC or DC which
42 sometimes limits its application. Zhang et al. [97] reported fabricating HEAs
43 with CO₂ laser, and the alloy had fine microstructural morphologies and higher
44 mechanical properties. While Zheng et al. [98] mentioned that the HEAs coat-
45 ing fabricated using gas lasers had cellular crystals with dispersion precipitates
46 although the hardness values were reported to be high [99].

47 b. Excimer lasers, on the other hand, is a mixture of noble gases like helium
48 buffer gas, xenon, argon and a chloride or fluoride halogen. Excimer which is

01 about 248 nm is also known as excited dimers which are pumped using a pulsed
02 electrical discharge for the production of nanosecond pulses in an ultraviolet
03 region, for that reason; it can only be operated in a pulsed mode. Other limita-
04 tions of this laser are low beam quality, the severity of maintenance and high
05 running cost [100]. Sharma et al. [101] reported using an excimer laser with a
06 wavelength of 248 nm for target ablation during the creation of epitaxial single
07 crystal high entropy ABO₃ perovskite thin films. The authors described how
08 this process was significant in understanding different bonding environments
09 to develop macroscopic responses driven by complex exchange interactions and
10 electron–phonon channels.

11 c. Nd:Yag which is an acronym for neodymium-doped yttrium aluminum garnet
12 laser is a 1064 nm solid-state laser made up of an active ion and a host from
13 either glass or solid crystalline. It is one of the widely used for the surface mod-
14 ification of HEAs attributed to the ability of its light beam to be transported
15 by flexible optical fibers, consequently increasing its delivery efficiency and
16 compactness [102, 103]. It is also not limited by its mode of transport, which
17 can occur both in pulse and continuous modes. Recently, diode lasers have been
18 substituted for Xenon flash lamps as the pump source to improve the quality of
19 the beam. More so, Nd: YVO₄ is a recent substitute for the Nd:Yag laser due to
20 its wider band absorption, high efficiency and lower operating threshold [104].

21 d. A Fiber Laser is about 848 nm in wavelength with a rare earth doped fiber
22 used for high power generation due to its increased level of efficiency. The
23 Yb-Doped fiber lasers have excellent electrical-to-optical efficiency with
24 system compactness and high-quality beam. Neodymium, holmium, thulium,
25 dysprosium, erbium and praseodymium are other rare earth elements used
26 as a gain medium in fiber lasers. Fiber lasers are usually pumped with laser
27 diodes; however, they are limited by their light propagation through the optical
28 fiber which greatly influences the guiding medium compared with when the
29 propagation occurs through the air inside the fiber. More so, other factors like
30 the Kerr lens and Raman effects limit the performance of the laser, therefore,
31 optical fibers with polarization maintenance are strongly recommended as
32 the gain medium [105]. Fan et al. [106] examined the influence of fiber laser
33 welding on the mechanical and microstructural proprieties in addition to the
34 solute segregation of a high entropy alloy. The authors reported that the alloy
35 showed dendritic structures with those fabricated using Nd:Yag laser and they
36 observed copper's segregation to the interdendritic region were also attributed
37 to its smaller bonding energies with other elements in the HEA composition,
38 conversely; the alloy showed better hardness and strength compared with
39 the Nd:Yag.

40 e. Organic liquid dye lasers use organic dyes as the gain medium. These liquid dye
41 with about 50–100 nm compared to solids have a higher density of atoms and
42 they are evenly distributed. These lasers with wide bandwidth are replaceable
43 and are transferred from very intricate regions which are sometimes used as
44 solutes in considerable solvents to develop gain mediums [107]. Coumarin,
45 pyrromethene, exalite, pyridine, styryl and fluorescein are dyes used for pulsed
46 or tunable lasers. Nevertheless, these lasers are limited in applications because
47 they require a large volume of organic solvents for efficiency. Xu et al. [108]
48 used a laser stimulated fluorescence equipment consisting of an organic liquid
49 dye to fabricate a HEA and study the performance of the coatings then the
50 influence of aluminum on the properties of the alloy. The authors stated that

01 the laser technology and the aluminum content enabled the phase transitions,
02 grain refinement and corrosion resistance observed.

03 f. Other types of lasers are; semiconductor lasers, hybrid laser arc welding and
04 free-electron lasers and the fabrications of HEAs using these lasers are limited
05 in research, hence, should be further explored.

06 **4.1 Laser surface melting (LSM)**

07 This type of surface modification is used for material hardening, electrochemi-
08 cal and tribological resistance and reduction in porosity. An increased rate of heat
09 transfer occurs during the interaction between the substrate and the melted HEAs
10 coating surface, especially during solidification. The rapid solidification and cool-
11 ing rates invariably produce fine microstructures which also enhances the surface
12 properties of the alloys. Chen et al. [109] used LSM on HEAs and they mentioned
13 that the surface modification process increased the electrochemical and mechani-
14 cal properties of the alloys. Ochelik et al. [105] found that the solidification rate
15 influences the phases formed using LSM. The fast solidification rates promoted the
16 BCC phase observed which was also responsible for the improved hardness proper-
17 ties of the alloys. Cai et al. [110] also reported observing a BCC solid solution phase
18 and improved microhardness properties after using LSM. The as-remelted HEAs
19 coatings had low wear mass loss showing an improvement in the wear resistance.

20 **4.2 Laser transformation hardening (LTH)**

21 The LTH heats the HEAs coating or films at a very high temperature with an
22 unfocused beam, and then rapid cooling occurs immediately without letting
23 equilibrium phases to form by quenching, as a result, generating very low thermal
24 distortion. This method uses a diode laser or CO₂ to increase the surface properties
25 of the HEAs [111].

26 **4.3 Laser surface alloying (LSA)**

27 This involves the direct injection or pre-placement of additional elements unto
28 the surface of the substrate by a laser source. Rapid solidification occurs with the
29 substrate maintaining its temperature while acting as a heat sink, still the composi-
30 tion of the surface changes [112]. Therefore, re-solidification and rapid quenching
31 follow due to the temperature difference between the surface of the substrate and
32 the treated surface zone. Zhang et al. [113] fabricated HEA coatings by LSA, and the
33 HEA coating had a BCC solid solution phase with improved mechanical and corro-
34 sion properties. Jiang et al. [114] fabricated HEAs on a 304 stainless steel substrate
35 and they stated that although the alloy had FCC and BCC phases, the BCC phase was
36 more predominant. The authors also recorded a substantial increase in the hardness
37 with good wear-resistant properties.

38 **4.4 Laser glazing**

39 This method produces a nanocrystalline layer or thin amorphous layer on the
40 surface of the substrate, energy is absorbed into the surface which melts the HEAs
41 coating/films to a certain depth with a laser beam and rapid solidification occurs.
42 This process is achieved using a high power density at a short period enough to cre-
43 ate the amorphous structure needed for surface modification [115].

01 5. Conclusion

02 High-temperature properties of materials used for turbine engine applications
03 are important for the reduction of fuel consumption, operating costs and pollution.
04 Nickel-based superalloys are widely used due to its strength, resistance to degrada-
05 tion in oxidizing environments, toughness and density. However, Nickel superalloy
06 is not stable at elevated temperatures having a maximum service temperature of
07 649 °C , the superalloy at room temperature has a negative lattice misfit, poor
08 thermal conductivity and difficult to machine. High Entropy Superalloys, with
09 similar γ and γ' phases as the Nickel-based superalloys, shows high tensile strength
10 than Inconel 617 and Alloy 800 H. The superalloy exhibits good oxidation resis-
11 tance; have lower densities below 8 g/cm³, a positive lattice misfit and high yield
12 strength compared to traditional nickel superalloys. Controlling the elemental
13 compositional partitioning between the γ - γ' in high entropy superalloys makes the
14 thermal stability higher than conventional nickel superalloys and equimolar or near
15 equimolar high entropy alloys. Therefore γ' precipitate strengthening of solid
16 solution high entropy alloys to form High Entropy Superalloys is currently the most
17 promising material for turbine engine applications. Laser surface modification
18 treatments can be used as a protective mechanism for Superalloys.

19 Acknowledgements

20 The authors will like to appreciate the National Laser Center (Laser Enabled
21 Manufacturing Resource Group); Council for Scientific and Research (CSIR) and
22 the Surface Engineering Research Laboratory; Tshwane University of Technology,
23 Pretoria, South Africa for their scientific and technical support during this research.

24 Author details

25 Modupeola Dada^{1*}, Patricia Popoola¹, Samson Adeosun², Sisa Pityana¹,
26 Ntombizodwa Mathe¹, Olufemi Aramide¹, Nicholus Malatji¹, Thabo Lengopeng¹
27 and Afolabi Ayodeji³


28 ¹ Chemical, Metallurgical and Materials Engineering, Tshwane University of
29 Technology, Pretoria, South Africa

30 ² Metallurgical and Materials Engineering, University of Lagos, Lagos, Nigeria

31 ³ Tshwane University of Technology, Pretoria, South Africa

32 *Address all correspondence to: dadadupeola@gmail.com

IntechOpen

© 2021 The Author(s). Licensee IntechOpen. This chapter is distributed under the terms of the Creative Commons Attribution License (<http://creativecommons.org/licenses/by/3.0>), which permits unrestricted use, distribution, and reproduction in any medium, provided the original work is properly cited. 

References

- 01 [1] Boyce, M.P., *Gas turbine engineering*
02 *handbook*. 2011: Elsevier. 41
- 03 [2] Kaygusuz, K., *Sustainable*
04 *development of hydroelectric power*.
05 Energy sources, 2002. **24**(9): p. 803-815. 42
- 06 [3] Langston, L.S., G. Opdyke, and E.
07 Dykewood, *Introduction to gas turbines*
08 *for non-engineers*. Global Gas Turbine
09 News, 1997. **37**(2): p. 1-9. 43
- 10 [4] Heywood, J.B., *Internal combustion*
11 *engine fundamentals*. 2018: McGraw-Hill
12 Education. 44
- 13 [5] Bell, M. and T. Partridge,
14 *Thermodynamic design of a reciprocating*
15 *Joule cycle engine*. Proceedings of the
16 Institution of Mechanical Engineers,
17 Part A: Journal of Power and Energy,
18 2003. **217**(3): p. 239-246. 45
- 19 [6] Cheng, C.-Y. and C.O.-K. Chen,
20 *Power optimization of an irreversible*
21 *Brayton heat engine*. Energy sources,
22 1997. **19**(5): p. 461-474. 46
- 23 [7] Viteri, F. and R.E. Anderson, *Semi-*
24 *closed brayton cycle gas turbine power*
25 *systems*. 2003, Google Patents. 47
- 26 [8] Walsh, P.P. and P. Fletcher, *Gas*
27 *turbine engine*. 2005, Google Patents. 48
- 28 [9] Li, Y. and P. Nilkitsaranont, *Gas*
29 *turbine performance prognostic for*
30 *condition-based maintenance*. Applied
31 energy, 2009. **86**(10): p. 2152-2161. 49
- 32 [10] Reed, R.C., *The superalloys:*
33 *fundamentals and applications*. 2008:
34 Cambridge university press. 50
- 35 [11] Liu, C., et al., *Improved castability*
36 *of directionally solidified, Ni-based*
37 *superalloy by the liquid metal cooling*
38 *process*. Metallurgical and Materials
39 Transactions A, 2012. **43**(2): p.
40 405-409. 51
- [12] Wang, R.-Z., et al., *Creep-fatigue*
life prediction and interaction diagram
in nickel-based GH4169 superalloy at
650 C based on cycle-by-cycle concept.
International Journal of Fatigue, 2017.
97: p. 114-123. 42
- [13] Ganji, D.K. and G. Rajyalakshmi,
Influence of Alloying Compositions on the
Properties of Nickel-Based Superalloys: A
Review, in *Recent Advances in Mechanical*
Engineering. 2020, Springer. p. 537-555. 47
- [14] Akca, E. and A. Gürsel, *A review*
on superalloys and IN718 nickel-based
INCONEL superalloy. Periodicals of
engineering and natural sciences,
2015. **3**(1). 48
- [15] Miracle, D.B., et al., *Refractory*
high entropy superalloys (RSAs). Scripta
Materialia, 2020. **187**: p. 445-452. 49
- [16] Tsao, T.-K., et al., *High temperature*
oxidation and corrosion properties of
high entropy superalloys. Entropy, 2016.
18(2): p. 62. 50
- [17] Yeh, A., et al., *Developing new type*
of high temperature alloys-high entropy
superalloys. International Journal of
Metallurgical & Materials Engineering,
2015. **2015**. 51
- [18] Pint, B.A., K. Unocic, and
S. Dryepondt. *Oxidation of*
superalloys in extreme environments.
in *7th International Symposium on*
Superalloy. 2010. 52
- [19] Liu, X., et al., *Effects of Nb and*
W additions on the microstructures and
mechanical properties of novel γ/γ' Co-
V-Ti-Based superalloys. Metals, 2018.
8(7): p. 563. 53
- [20] Locq, D., et al., *Development of*
new PM superalloys for high temperature
applications. Intermetallics and
superalloys, 2000. **10**: p. 52-57. 54

- 01 [21] Graybill, B., et al. *Additive*
02 *Manufacturing of nickel-based*
03 *superalloys*. in *International*
04 *Manufacturing Science and Engineering*
05 *Conference*. 2018. American Society of
06 Mechanical Engineers.
- 07 [22] Walston, S., et al., *Joint development*
08 *of a fourth generation single crystal*
09 *superalloy*. 2004.
- 10 [23] Perrut, M., et al., *High temperature*
11 *materials for aerospace applications:*
12 *Ni-based superalloys and γ -TiAl alloys*.
13 *Comptes Rendus Physique*, 2018. **19**(8):
14 p. 657-671.
- 15 [24] Gessinger, G.H. and M. Bomford,
16 *Powder metallurgy of superalloys*.
17 *International Metallurgical Reviews*,
18 1974. **19**(1): p. 51-76.
- 19 [25] Bewlay, B., et al., *Net-shape*
20 *manufacturing of aircraft engine disks by*
21 *roll forming and hot die forging*. *Journal of*
22 *Materials Processing Technology*, 2003.
23 **135**(2-3): p. 324-329.
- 24 [26] Lavella, M., T. Berruti, and E.
25 Bosco, *Residual stress analysis in Inconel*
26 *718 milled turbine disk*. *International*
27 *Journal of Machining and Machinability*
28 *of Materials*, 2008. **4**(2-3): p. 181-194.
- 29 [27] Groh, J., et al. *Development of a*
30 *new cast and wrought alloy (René 65)*
31 *for high temperature disk applications*.
32 in *Proceedings of the 8th International*
33 *Symposium on Superalloy 718 and*
34 *Derivatives*. 2014. John Wiley & Sons.
- 35 [28] Pollock, T.M. and S. Tin, *Nickel-*
36 *based superalloys for advanced turbine*
37 *engines: chemistry, microstructure and*
38 *properties*. *Journal of propulsion and*
39 *power*, 2006. **22**(2): p. 361-374.
- 40 [29] Ezugwu, E., J. Bonney, and
41 Y. Yamane, *An overview of the*
42 *machinability of aeroengine alloys*.
43 *Journal of materials processing*
44 *technology*, 2003. **134**(2): p. 233-253.
- [30] Reed, R., T. Tao, and N. Warnken, 45
Alloys-by-design: application to nickel- 46
based single crystal superalloys. *Acta* 47
Materialia, 2009. **57**(19): p. 5898-5913. 48
- [31] Kennedy, R., *ALLVAC® 718PLUS™,* 49
superalloy for the next forty years. 50
Superalloys, 2005. **718**(706): p. 1-14. 51
- [32] Devaux, A., et al., *AD730TM-A* 52
new nickel-based superalloy for high 53
temperature engine rotative parts. *TMS* 54
Superalloys, 2012. **911919**. 55
- [33] Thellaputta, G.R., P.S. Chandra, 56
and C. Rao, *Machinability of nickel* 57
based superalloys: a review. *Materials* 58
Today: Proceedings, 2017. **4**(2): p. 59
3712-3721. 60
- [34] Flower, H.M., *High performance* 61
materials in aerospace. 2012: Springer 62
Science & Business Media. 63
- [35] Lehockey, E., G. Palumbo, and P. 64
Lin, *Improving the weldability and service* 65
performance of nickel-and iron-based 66
superalloys by grain boundary engineering. 67
Metallurgical and materials transactions 68
a, 1998. **29**(12): p. 3069-3079. 69
- [36] Durand-Charre, M., *The* 70
microstructure of superalloys. 2017:
71
Routledge. 72
- [37] Sikka, V., et al., *Advances in* 73
processing of Ni3Al-based intermetallics 74
and applications. *Intermetallics*, 2000.
75 **8**(9-11): p. 1329-1337. 76
- [38] Frank, R.B., C.G. Roberts, and 77
J. Zhang. *Effect of nickel content* 78
on delta solvus temperature and 79
mechanical properties of alloy 718.
80 in *7th international symposium on*
81 *superalloy*. 2010. 82
- [39] Choudhury, I. and M. El-Baradie, 83
Machinability of nickel-base super alloys: 84
a general review. *Journal of Materials* 85
Processing Technology, 1998. **77**(1-3): 86
p. 278-284. 87

- 01 [40] Gao, M.C. and D.E. Alman, *Searching for next single-phase high-* 44
 02 *entropy alloy compositions.* Entropy, 2013. 45
 03 **15**(10): p. 4504-4519. [51] Mishra, R.K. and R.R. Shahi, 46
 04 *Magnetic characteristics of high entropy* 47
 05 [41] Chatterjee, P., V.M. Athawale, and 48
 06 S. Chakraborty, *Selection of materials* 49
 07 *using compromise ranking and outranking* 50
 08 *methods.* Materials & Design, 2009. 51
 09 **30**(10): p. 4043-4053. [52] Senkov, O., et al., *Refractory high-* 52
 10 [42] Chen, J., et al., *A review on* 53
 11 *fundamental of high entropy alloys with* 54
 12 *promising high-temperature properties.* 55
 13 *Journal of Alloys and Compounds,* 2018. 56
 14 **760**: p. 15-30. [53] Hemphill, e.a., *Fatigue behavior* 57
 15 [43] Hummel, R.E., *Understanding* 58
 16 *materials science: history, properties,* 59
 17 *applications.* 2004: Springer Science & 60
 18 Business Media. [54] Tsao, T.-K., et al., *The high* 61
 19 [44] Cantor, B., et al., *Microstructural* 62
 20 *development in equiatomic* 63
 21 *multicomponent alloys.* Materials Science 64
 22 and Engineering: A, 2004. **375**: p. 65
 23 213-218. [55] Senkov, O.N., et al., *Development* 66
 24 [45] Ye, Y., et al., *High-entropy alloy:* 67
 25 *challenges and prospects.* Materials Today, 68
 26 2016. **19**(6): p. 349-362. [56] Chen, Y.-T., et al., *Hierarchical* 65
 27 [46] Yeh, J.W., et al., *Nanostructured high-* 66
 28 *entropy alloys with multiple principal* 67
 29 *elements: novel alloy design concepts* 68
 30 *and outcomes.* Advanced Engineering 69
 31 Materials, 2004. **6**(5): p. 299-303. [57] Tsao, T.-K., A.-C. Yeh, and H. 70
 32 [47] Joseph, J., *Study of direct laser* 71
 33 *fabricated high entropy alloys.* 2016, 72
 34 Deakin University. Murakami, *The microstructure stability of* 73
 35 [48] Kuehl, R.O. and R. Kuehl, *Design* 74
 36 *of experiments: statistical principles of* 75
 37 *research design and analysis.* 2000. [58] Daoud, H., et al., *Microstructure and* 76
 38 [49] Wang, Y.P., B.S. Li, and H.Z. Fu, 77
 39 *Solid solution or intermetallics in a high-* 78
 40 *entropy alloy.* Advanced engineering 79
 41 materials, 2009. **11**(8): p. 641-644. [59] He, J., et al., *A precipitation-hardened* 80
 42 [50] Gludovatz, B., et al., *A fracture-* 81
 43 *resistant high-entropy alloy for cryogenic* 82
applications. Science, 2014. **345**(6201): 83
 p. 1153-1158. [60] Zhao, Y., et al., *Thermal stability* 84
and coarsening of coherent particles in 85
a precipitation-hardened (NiCoFeCr)

- 01 94Ti2Al4 high-entropy alloy. Acta
02 Materialia, 2018. **147**: p. 184-194.
- 03 [61] Xiao, K., et al., *A scanning AC*
04 *calorimetry technique for the analysis of*
05 *nano-scale quantities of materials*. Review
06 of Scientific Instruments, 2012. **83**(11):
07 p. 114901.
- 08 [62] Wang, Z., et al., *Effect of coherent*
09 *L12 nanoprecipitates on the tensile*
10 *behavior of a fcc-based high-entropy alloy*.
11 Materials Science and Engineering: A,
12 2017. **696**: p. 503-510.
- 13 [63] Gwalani, B., et al., *Stability of*
14 *ordered L12 and B2 precipitates in*
15 *face centered cubic based high entropy*
16 *alloys-Al0.3CoFeCrNi and Al0.3*
17 *3CuFeCrNi2*. Scripta Materialia, 2016.
18 **123**: p. 130-134.
- 19 [64] Borkar, T., et al., *A combinatorial*
20 *assessment of AlxCrCuFeNi2 (0 <*
21 *x < 1.5) complex concentrated alloys:*
22 *Microstructure, microhardness, and*
23 *magnetic properties*. Acta Materialia,
24 2016. **116**: p. 63-76.
- 25 [65] Li, Y., et al., *Microstructure and*
26 *elevated-temperature mechanical*
27 *properties of refractory AlMo0.5NbTa0.5*
28 *TiZr High Entropy Alloy fabricated*
29 *by powder metallurgy*. arXiv preprint
30 arXiv:1801.00263, 2017.
- 31 [66] Kai, W., et al., *The oxidation*
32 *behavior of a Ni2FeCoCrAl0.5 high-*
33 *entropy superalloy in O2-containing*
34 *environments*. Corrosion Science, 2019.
35 **158**: p. 108093.
- 36 [67] Shafiee, A., et al., *Development and*
37 *microstructural characterization of a new*
38 *wrought high entropy superalloy*. Metals
39 and Materials International, 2019:
40 p. 1-12.
- 41 [68] Saito, T., et al., *Effect of Heat*
42 *Treatments on the Microstructural*
43 *Evolution of a Single Crystal High-*
44 *Entropy Superalloy*. Metals, 2020. **10**(12):
45 p. 1600.
- [69] Zhang, L., et al., *Microstructure and*
mechanical properties of precipitation-
hardened cast high-entropy superalloys.
Materials Science and Technology,
2020: p. 1-7.
- [70] Belan, J., *GCP and TCP phases*
presented in nickel-base superalloys.
Materials Today: Proceedings, 2016.
3(4): p. 936-941.
- [71] Yeh, A.-c. and T.-K. Tsao, *High-*
entropy superalloy. 2019, Google Patents.
- [72] Zhang, J., et al., *The effect of*
lattice misfit on the dislocation motion
in superalloys during high-temperature
low-stress creep. Acta Materialia, 2005.
53(17): p. 4623-4633.
- [73] Mughrabi, H., *The importance of*
sign and magnitude of γ/γ' lattice misfit
in superalloys—with special reference
to the new γ' -hardened cobalt-base
superalloys. Acta materialia, 2014. **81**:
p. 21-29.
- [74] Chawla, V., et al., *Corrosion*
Behavior of Nanostructured TiAlN
and AlCrN Hard Coatings on Superfer
800H Superalloy in Simulated Marine
Environment. Journal of Minerals
and Materials Characterization and
Engineering, 2009. **8**(9): p. 693-700.
- [75] Sidhu, T., et al., *Oxidation and*
hot corrosion resistance of HVOF
WC-NiCrFeSiB coating on Ni-and
Fe-based superalloys at 800 C. Journal of
Thermal Spray Technology, 2007. **16**(5-
6): p. 844-849.
- [76] Moody, N., et al., *Temperature*
effects on hydrogen-induced crack growth
susceptibility of iron-based superalloys.
Engineering Fracture Mechanics, 2001.
68(6): p. 731-750.
- [77] Chung, D.-W., et al., *Effects of Cr*
on the properties of multicomponent
cobalt-based superalloys with ultra high
 γ' volume fraction. Journal of Alloys and
Compounds, 2020: p. 154790.

- 01 [78] Makineni, S., B. Nithin, and K. 45
 02 Chattopadhyay, *Synthesis of a new 46*
 03 *tungsten-free γ - γ' cobalt-based superalloy 47*
 04 *by tuning alloying additions*. Acta
 05 Materialia, 2015. **85**: p. 85-94.
- 06 [79] Peters, M., et al., *Titanium alloys 50*
 07 *for aerospace applications*. Advanced
 08 engineering materials, 2003. **5**(6): p. 51
 09 419-427. Springer. p. 1-87.
- 10 [80] Clemens, H. and W. Smarsly. *Light- 54*
 11 *weight intermetallic titanium aluminides- 55*
 12 *status of research and development*. in
 13 *Advanced materials research*. 2011. Trans 57
 14 Tech Publ. Compounds, 2017. **698**: p. 761-770. 58
- 15 [81] Wee, S., et al., *Review on Mechanical 59*
 16 *Thermal Properties of Superalloys and 60*
 17 *Thermal Barrier Coating Used in Gas 61*
 18 *Turbines*. Applied Sciences, 2020. 62
 19 **10**(16): p. 5476. Technology, 2015. **262**: p. 64-69. 63
- 20 [82] Goward, G.W., *Current research on 64*
 21 *the surface protection of superalloys for 65*
 22 *gas turbine engines*. JOM, 1970. **22**(10): 66
 23 p. 31-39. p. 338-343. 68
- 24 [83] Couturier, R. and C. Escaravage, 69
 25 *High temperature alloys for the HTGR 70*
 26 *Gas Turbine: Required properties and 71*
 27 *development needs*. 2001. Metallography, Microstructure, and 72
 28 [84] Sims, C.T., N.S. Stoloff, and W.C. 73
 29 Hagel, *superalloys II*. 1987: Wiley
 30 New York. Analysis, 2016. **5**(3): p. 229-240.
- 31 [85] Zhu, S. and F. Wang, 74
 32 *Nanocrystalline, Enamel and Composite 75*
 33 *Coatings for Superalloys*, in *Production, 76*
 34 *Properties, and Applications of High 77*
 35 *Temperature Coatings*. 2018, IGI Global. 78
 36 p. 160-186. p. 177-184.
- 37 [86] Levi, C.G., *Emerging materials and 79*
 38 *processes for thermal barrier systems*. 80
 39 Current Opinion in Solid State and 81
 40 Materials Science, 2004. **8**(1):
 41 p. 77-91. 355-372.
- 42 [87] Goward, G., *Progress in coatings for 82*
 43 *gas turbine airfoils*. Surface and coatings 83
 44 technology, 1998. **108**: p. 73-79. 84
 85
 86
- [88] Galetz, M.C., *Coatings for 87*
superalloys, in *Superalloys*. 2015, InTech. 88
 p. 277-298.
- [89] Chatterji, D., R. DeVries, and G. 48
 Romeo, *Protection of superalloys for 49*
turbine application, in *Advances in 50*
corrosion science and technology. 1976, 51
 Springer. p. 1-87. 52
- [90] Wu, C., et al., *Phase evolution and 53*
cavitation erosion-corrosion behavior 54
of FeCoCrAlNiTi_x high entropy alloy 55
coatings on 304 stainless steel by laser 56
surface alloying. Journal of Alloys and 57
 Compounds, 2017. **698**: p. 761-770. 58
- [91] Zhang, S., et al., *Synthesis and 59*
characterization of FeCoCrAlCu 60
high-entropy alloy coating by laser 61
surface alloying. Surface and Coatings 62
 Technology, 2015. **262**: p. 64-69. 63
- [92] Huang, C., et al., *Dry sliding wear 64*
behavior of laser clad TiVCrAlSi high 65
entropy alloy coatings on Ti-6Al-4V 66
substrate. Materials & Design, 2012. **41**: 67
 p. 338-343. 68
- [93] Nahmany, M., et al., *Al_xCrFeCoNi 69*
High-Entropy Alloys: Surface Modification 70
by Electron Beam Bead-on-Plate Melting. 71
 Metallography, Microstructure, and 72
 Analysis, 2016. **5**(3): p. 229-240. 73
- [94] Tian, Y., et al., *Research progress on 74*
laser surface modification of titanium 75
alloys. Applied Surface Science, 2005. 76
242(1-2): p. 177-184. 77
- [95] Herd, R.M., J.S. Dover, and 78
 K.A. Arndt, *Basic laser principles. 79*
 Dermatologic clinics, 1997. **15**(3): p. 80
 355-372. 81
- [96] Natto, Z.S., et al., *Comparison of the 82*
efficacy of different types of lasers for the 83
treatment of peri-implantitis: a systematic 84
review. International Journal of Oral & 85
 Maxillofacial Implants, 2015. **30**(2). 86
- [97] Zhang, H., et al. *Synthesis and 87*
characterization of NiCoFeCrAl₃ high 88

- 01 *entropy alloy coating by laser cladding.* alloy. Journal of Laser Applications, 45
02 in *Advanced Materials Research*. 2010. 2020. **32**(2): p. 022005. 46
03 Trans Tech Publ.
- 04 [98] Zheng, B., Q.B. Liu, and L.Y. [107] Rekha, M., N. Mallik, and C. 47
05 Zhang. *Microstructure and properties* Srivastava, *First report on high entropy* 48
06 *of MoFeCrTiW high-entropy alloy* alloy nanoparticle decorated graphene. 49
07 *coating prepared by laser cladding.* Scientific reports, 2018. **8**(1): p. 1-10. 50
08 *Advanced Materials Research*. 2013. Trans [108] Xu, Y., et al., *Microstructure* 51
09 Tech Publ. *Evolution and Properties of Laser* 52
Cladding CoCrFeNiTiAlx High-Entropy 53
Alloy Coatings. Coatings, 2020. 54
10 [99] Ye, X., et al., *The property research* **10**(4): p. 373. 55
11 *on high-entropy alloy AlxFeCoNiCuCr*
12 *coating by laser cladding.* Physics [109] Chen, C., et al., *Influences of* 56
13 *Procedia*, 2011. **12**: p. 303-312. *laser surface melting on microstructure,* 57
mechanical properties and corrosion 58
resistance of dual-phase Cr-Fe-Co-Ni-Al 59
high entropy alloys. Journal of Alloys and 60
14 [100] Guo, X., et al., *Corrosion behavior* *Compounds*, 2020. **826**: p. 154100. 61
15 *of aluminum in fluoride-containing*
16 *discharge condition for excimer laser*
17 *structure application.* Materials Research [110] Cai, Z., et al., *Microstructure and* 62
18 *Express*, 2019. **6**(10): p. 106519. *wear resistance of laser clad Ni-Cr-* 63
Co-Ti-V high-entropy alloy coating after 64
laser remelting processing. Optics & Laser [111] Ion, J., *Laser transformation* 67
19 [101] Sharma, Y., et al., *Magnetic* *hardening.* Surface engineering, 2002. 68
20 *anisotropy in single-crystal high-entropy* **18**(1): p. 14-31. 69
21 *perovskite oxide La (Cr 0.2 Mn 0.2*
22 *Fe 0.2 Co 0.2 Ni 0.2) O 3 films.* Physical Review Materials, 2020. **4**(1):
23 p. 014404.
24 [102] Dobbstein, H., et al., *Direct metal*
25 *deposition of refractory high entropy alloy*
26 *MoNbTaW.* Physics Procedia, 2016. **83**:
27 p. 624-633.
28 [103] Nam, H., et al., *Effect of post*
29 *weld heat treatment on weldability of*
30 *high entropy alloy welds.* Science and
31 *Technology of Welding and Joining*,
32 2018. **23**(5): p. 420-427.
33 [104] Rafique, M.M.A., *Additive*
34 *Manufacturing of Bulk Metallic Glasses*
35 *and their composites—Recent trends and*
36 *approaches.*
37 [105] Ocelík, V., et al., *Additive*
38 *manufacturing of high-entropy alloys*
39 *by laser processing.* Jom, 2016. **68**(7): p.
40 1810-1818.
41 [106] Fan, Y., et al., *Effect of fiber*
42 *laser welding on solute segregation and*
43 *properties of CoCrCuFeNi high entropy*
44 *alloy.* Journal of Laser Applications, 45
2020. **32**(2): p. 022005. 46
[107] Rekha, M., N. Mallik, and C. 47
Srivastava, *First report on high entropy* 48
alloy nanoparticle decorated graphene. 49
Scientific reports, 2018. **8**(1): p. 1-10. 50
[108] Xu, Y., et al., *Microstructure* 51
Evolution and Properties of Laser 52
Cladding CoCrFeNiTiAlx High-Entropy 53
Alloy Coatings. Coatings, 2020. 54
10(4): p. 373. 55
[109] Chen, C., et al., *Influences of* 56
laser surface melting on microstructure, 57
mechanical properties and corrosion 58
resistance of dual-phase Cr-Fe-Co-Ni-Al 59
high entropy alloys. Journal of Alloys and 60
Compounds, 2020. **826**: p. 154100. 61
[110] Cai, Z., et al., *Microstructure and* 62
wear resistance of laser clad Ni-Cr- 63
Co-Ti-V high-entropy alloy coating after 64
laser remelting processing. Optics & Laser [111] Ion, J., *Laser transformation* 67
hardening. Surface engineering, 2002. 68
18(1): p. 14-31. 69
[112] Manilal, K.M., et al., *A Review on* 70
Laser Surface Alloying. International 71
Research Journal of Engineering and 72
Technology, 2017. **4**(03): p. 4. 73
[113] Zhang, S., et al., *Laser surface* 74
alloying of FeCoCrAlNi high-entropy 75
alloy on 304 stainless steel to enhance 76
corrosion and cavitation erosion resistance. 77
Optics & Laser Technology, 2016. **84**:
p. 23-31. 78
79
[114] Jiang, P., et al., *Microstructure* 80
and Properties of CeO 2-Modified 81
FeCoCrAlNiTi High-Entropy Alloy 82
Coatings by Laser Surface Alloying. 83
Journal of Materials Engineering and 84
Performance, 2020: p. 1-10. 85
[115] Pawlowski, L., *Thick laser coatings:* 86
A review. Journal of thermal spray 87
technology, 1999. **8**(2): p. 279-295. 88